

# SUGGESTIVE CONTOURS OVER POINT-SET IMPLICITS

João Proença, Joaquim Jorge

*Department of Computer Systems Engineering, INESC-ID/IST/Technical, University of Lisbon, Portugal*

Mario Costa Sousa

*Department of Computer Science, University of Calgary, Canada*

**Keywords:** Implicit surfaces, point-based graphics, non-photorealistic rendering.

**Abstract:** This paper presents a system that combines large point-set implicit surfaces with fast line-based rendering. We devised a new process for extracting suggestive contours quickly by using particles scattered throughout the surface to identify areas of interest, followed by clustering and line-fitting. Furthermore, we improve on state-of-the-art methods for extracting silhouettes and feature-lines by harnessing the descriptive power of the surface representation. This provides heuristics for fast determination of curvature and allows for the local regeneration of shape-depicting line elements after editing operations. While visual examples illustrate the high quality of the drawings obtained with our application, as well as the high detail it can provide for more complex models, run-times show comparatively higher performance over similar approaches for the same number of points.

## 1 INTRODUCTION

Non-Photorealistic Rendering (NPR) methods are commonly used to depict the shape of three-dimensional objects in a way similar to the existing types of artistic drawing techniques. Recently, most of the work presented on real-time extraction of lines from 3D objects has focused mainly on polygonal meshes. However, even though meshes are visualization-friendly structures, they pose serious difficulties for shape modeling. Namely, memory usage increases with both shape size and detail, while it is difficult to maintain topological consistency with editing operations. There are other representations that are better suited for such operations and for which direct rendering techniques should be devised. One such representation is the implicit surface, which provides a simple and flexible mathematical definition that derives from a potential field function.

In this paper we present techniques to quickly extract shape-depicting lines from Multi-level Partition of Unity (MPU) implicits (Ohtake et al., 2003), which are able to represent complex surfaces from large sets of points. These techniques were applied directly to an already existing system (de Araujo and

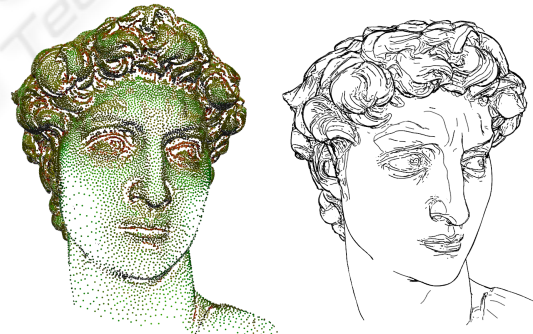


Figure 1: MPU surface computed with a relative error of  $5 \times 10^{-4}$ . Left: David's Head model with 59994 particles scattered over the surface. Right: The same model rendered with our system using silhouettes, suggestive contours and feature lines.

Jorge, 2004), which allows users to interactively edit complex objects defined by MPU implicits. The user is able to apply modeling operations through a calligraphic interface that converts 2D strokes into 3D shape modifications. The implementation of our techniques in such a system allowed us to use an already existing application and is justified by our motivation to use such rendering methods in an environment that

supports shape editing.

Our approach draws inspiration from methods presented in (Foster et al., 2005) to construct a particle system over an implicit surface, extract silhouettes and feature-lines starting from the positions of these scattered particles and then using surfels to remove hidden lines. However, their approach does not support suggestive contours and uses a different implicit representation (BlobTree), which supports object definition through constructive solid geometry (CSG). We were more interested in using the MPU since it allows representing complex models from very large sets of points, which can be obtained from 3D scanning of real objects. One of the other advantages of the MPU implicit is its associated octree structure (Ohtake et al., 2003) that establishes a 3D cell division of the surrounding space of the object, in which the cell subdivision level is higher in areas of higher complexity. We highlight the main contributions of our work below.

- We present a novel technique for extracting suggestive contours from implicit surfaces. This is done by identifying particles that lie in surface areas where a suggestive contour exists, clustering those and applying line-fitting algorithms. This process works even when the local curvature information is not well-behaved, making our technique generalizable to most implicit surface representations, not just MPUs.
- We use the MPU cell subdivision information as a heuristic that in many ways improves the performance and precision of both the particle system simulation and the line extraction process. Indeed, probing the hierarchical level of each cell allows us to heuristically determine line lengths for contours, which tend to be shorter in areas of higher detail (deeper cell levels) and longer in flatter regions (cells closer to octree root).
- We provide support for dynamic line-elements, by using the MPU octree to allow locally regenerating particles and view-independent lines at interactive speeds after shape editing operations, even in surfaces with tens of thousands of particles.

We also use the MPU octree to set the initial positions of particles throughout the surface, which provides an automatic process for choosing the number of particles that is adequate for each model without the need for user intervention, contrary to other methods (Foster et al., 2005) which use random placement and require manual adjustments as described in detail in a previous publication (Proena et al., 2007). All of these elements come together in one system that combines the expressiveness of line-based rendering

with the descriptive power of the MPU, to visualize and edit objects defined by very large sets of points.

## 2 RELATED WORK

Most of the developed NPR methods that include silhouette, feature-line or suggestive contour extraction focus on polygon meshes and have been gaining momentum steadily over the past few years (Isenberg et al., 2003; Gooch et al., 1999; Sousa et al., 2003; DeCarlo et al., 2003; DeCarlo et al., 2004; Judd et al., 2007). However, while there was some earlier efforts applied to NPR directly over implicit representations (Bremer and Hughes, 1998; Elber, 1998) only in more recent years have we seen a return to the subject (Plantinga and Vegter, 2003; Foster et al., 2005).

Bremer and Hughes (Bremer and Hughes, 1998) presented methods for rendering lines over implicit surfaces, which used ray-intersection to determine points over the surface and numerical integration processes to make them approach the silhouettes and follow them. The same type of ray-driven techniques were used for positioning short interior strokes and perform hidden-line removal (HLR). More recently, Foster et al. (Foster et al., 2005) proposed techniques that combined these methods with some of the ideas introduced by Elber (Elber, 1998), such as the usage of a Witkin-Heckbert particle system (Witkin and Heckbert, 1994) for scattering points over the surface instead of the more computationally demanding ray-intersection algorithms. Using a variation of the Shrink-wrap method (van Overveld and Wyvill, 2004), feature-lines are also extracted from particles through the identification of straddle points over surface faces. An additional HLR method that used surfels was also presented in that paper. In terms of the Witkin-Heckbert based particle systems, Levet et al. (Levet et al., 2006) recently presented a technique that relies on geometry processing for finding near-optimal initial positions for particles, which improves the subsequent simulation time, but their approach requires more complex calculations in this step than ours. (Jepp et al., 2006) also extended the development of the particle system in (Foster et al., 2005) to create smarticles that use flocking behaviour for feature searching and line drawing in implicit surfaces.

In terms of suggestive contours, they are a fairly recent concept that was introduced by DeCarlo et al. (DeCarlo et al., 2003; DeCarlo et al., 2004). These two papers cover the mathematical definitions for suggestive contours on a surface and their extraction from polygonal meshes. (DeCarlo et al., 2003) presents the formal definitions and two algorithmic

approaches for producing rendered images of 3D objects (one in object-space and the other in image-space). In (DeCarlo et al., 2004) the authors extend the previous system to render suggestive contours in real-time, using line-movement analysis techniques and fast algorithms for polygon elimination in the line-searching process. These papers set the standard for suggestive contour rendering over meshes, but there are not many papers that cover their extraction from other types of representations. (Burns et al., 2005) provides techniques for silhouette and suggestive contour extraction from volume data using auxiliary level-sets, but their methods seem more suited to volumetric rather than surface-only data such as ours. (Schmidt et al., 2006) attempts to draw this type of lines over implicits, but uses a low-resolution mesh as an intermediate step for the line-extracting algorithms, which can be a limiting factor for some scenarios. It was our goal to avoid using this type of approach because the process of reconstructing the mesh in CSG operations is not straightforward over an implicit. To the best of our knowledge no published papers cover suggestive contour extraction from implicits without resorting to a mesh.

Our approach uses the definitions for suggestive contours presented in (DeCarlo et al., 2003) to identify particles in the MPU surface, create clusters from those particles and form contour lines by the application of line-fitting algorithms to the clusters. This method was inspired by the work presented by (Barla et al., 2005), which applies geometric clustering algorithms to line drawing simplification. However, their methods are based on the premise that large sets of lines are already available for simplification, which is not our case. Furthermore, the technique operates in image-space, which would make it impossible to use our surfel-based HLR method for suggestive contours. Therefore our approach evolved to extracting curves that represent clustered sets of 3D points. (Gumhold et al., 2001) presented methods for feature extraction from point clouds, where minimum-spanning-trees are built over clusters of points and later trimmed to form the representative lines. Our main approach to cluster line-fitting adapted this method to the characteristics of suggestive contours, but other approaches that fitted smooth curves to sets of points were also considered detail in Section 5.3.

## 2.1 The MPU Surface

An implicit surface (Bloomenthal, 1997) is defined through the potential function  $f(\mathbf{x})$  as the set of points  $\mathbf{x}=(x,y,z)$  that respect the condition:

$$f(\mathbf{x}) = iso \quad (1)$$

where  $iso$  is a constant value. In our case, where  $iso=0$ , the negative or positive values of  $f(\mathbf{x})$  indicate that  $\mathbf{x}$  is inside or outside of the object volume respectively. Implicits by their own nature provide a compact and flexible definition for highly complex surfaces and make blending operations easy to apply.

The MPU (Ohtake et al., 2003) is one of the various of types of implicit surfaces, which stands out for providing a method for efficient model construction from a dense set of control points sampled on the surface of complex objects. Its structure is composed by three elements: an octree of cubic spatial cells that cover the object; quadratic functions that approximate the local shape in each cell and weight functions that blend the local functions, thus providing a precision-controllable approximation to a complex implicit surface efficiently. The construction of an MPU implicit is guided by the subdivision of the octree structure, where cells become smaller and more numerous in areas where the point positions and normals suggest a higher curvature. We have extended the model to support interactive shape-editing operations. The spatial enumeration allows us to mark the local MPU cells that are involved in an edit operation and reconstruct the MPU locally from a new set of control points, which greatly benefits system performance (de Araujo and Jorge, 2004).

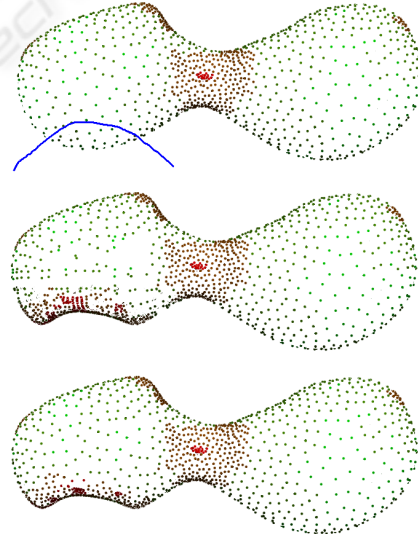


Figure 2: Shape editing. Top: The user defines a CSG cut over a simple object, using the blue 2D stroke. Center: The MPU surface is locally altered and new particles are generated in that area. Bottom: Particles become redistributed after a local simulation, which takes a few seconds.

### 3 OVERVIEW

Our methods follow a high-level approach similar to Foster et al. (Foster et al., 2005), in which particles are distributed across the surface. Silhouettes, suggestive contours and feature lines depicting surface discontinuities are then extracted from the relevant particles. However, while Foster et al. maintained the particle system in a constant simulation state (the particle positions are always being updated in a continuous cycle), we only let the simulation occur for a maximum number of iterations that are sufficient for an acceptable distribution of points throughout the surface. This results in a limited simulation time, after which a lot of computational resources are freed for the line-extracting algorithms. We also provide the users with the possibility of saving the particle system state to a file, allowing them to reuse it every time they load the same object in the application, without having to endure the simulation process again.

Silhouettes and suggestive contours are view-dependent elements, so we regenerate them whenever there is a change in the viewing conditions or whenever the particle system is in a simulation state. Feature lines depicting geometric-dependent discontinuities are view-independent (sometimes they are also called ridge and valley lines), so we only generate them once after some iterations of the particle system and then apply the appropriate 3D transformations whenever the viewing conditions change.

Foster et al. treat the implicit representation as a black-box, i.e. their methods only query the potential function to extract its value and gradient, making their approach usable with almost any type of implicit. While our approach requires the same mathematical information, we exploit the spatial information provided by the octree, thus leveraging on the data structures associated with the MPU. This includes using its octree for particle and line proximity, instead of using a regular grid as in their method.

Our system supports modeling operations via a calligraphic interface (de Araujo and Jorge, 2004). After an editing operation, we mark the affected octree cells and start a new particle system simulation confined to those cells. This makes the regeneration of particles much more efficient, because only the local particles are affected. This is illustrated in Figure 2, in which we can clearly see the redistribution of particles after editing the surface shape. Since feature-lines are view-independent elements, they are also locally regenerated. While our work was mainly concerned with rendering implicit surfaces, it is important to ensure that shape editing is still possible and efficient with our techniques, because it is one

of the main motivations for using implicits instead of other representations, especially in the MPU where the local reconstruction of surface areas is directly supported in CSG and blending operations.

Finally, to perform hidden line removal we use a surfel approach, as in (Foster et al., 2005). Surfels are oriented ellipses or circles which are used for point-based rendering of surfaces (Pfister et al., 2000). Our approach uses circular textures inside quadrilateral polygons positioned slightly behind each particle using the surface normal for orientation. These are rendered as white disks and have a radius set by the distance to the nearest particle. Although this method does not guarantee a total occlusion for all cases, it is very effective as long as we have a good distribution of particles throughout the surface.

### 4 THE PARTICLE SYSTEM

Our particle system improves on the approach of Foster et al., which is based on Witkin and Heckbert's (Witkin and Heckbert, 1994) model. While their methods place particles at random initial positions, we use the MPU features to obtain a better initial distribution as described in (Proena et al., 2007), which we recall here to help in understanding what follows. Our objective is to achieve denser concentrations of particles in areas of higher surface curvature. Since octree cells are smaller and more numerous in those areas, we create  $k$  random particles in each cell, where  $k$  is fixed (usually  $k = 1$ ), and obtain an initial distribution that is already close to our final objective, thus saving a considerable number of simulation iterations. We obtain a set of  $n$  particles,  $P_i, i \in [1, n]$ , chosen from the set of MPU control-points that already lie on the surface. Each of these particles is registered in the corresponding octree cell, enabling us to use fast algorithms for point-proximity determinations, using nearby-cell inspection.

The particle system simulation process is composed by a set of iterations where, at each step every particle suffers attraction and repulsion forces and moves accordingly. The calculation of these forces, as well as the movement of each particle, is performed in the same way as in (Foster et al., 2005), with the difference that we compute the repulsion distribution factor  $\delta_i$  in a different way. This value directly influences the repulsion force and controls the local density of particles. Foster et al. calculate this using Hessian values extracted from the potential function to determine the local mean curvature. This poses a significant computational burden; we avoid this altogether by using the octree cell depth information on

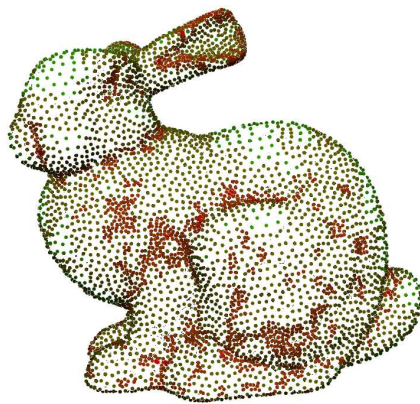


Figure 3: 10000 particles scattered over the surface of the Bunny model, after running 20 iterations of the particle system simulation. Red points correspond to octree cells of higher depth, green points to lower depth.

the MPU. The depth indicates the cell subdivision degree and therefore is a good heuristic for determining local curvature, which yields a simpler formula for  $\delta_i$ :

$$\delta_i = \text{weight}\left(\frac{d_i - d_{\min}}{d_{\max} - d_{\min}}\right) \quad (2)$$

where  $d_i$  is the cell depth of particle  $P_i$  and  $d_{\max}$  and  $d_{\min}$  are the maximum and minimum cell depths where particles exist in the model (these are determined during the initial particle generation step). The *weight* function is a quadratic B-Spline that sets a higher value for  $\delta_i$  if the particle is in one of the lower depth cells (less curved regions of the surface) and vice versa. The practical effect of using this technique is that it is easy and fast to obtain good results where the particles become well distributed over the surface to reflect local curvature with comparatively less steps and a lower cost per particle (see Figures 1 and 3).

## 5 SUGGESTIVE CONTOURS

Suggestive contours (DeCarlo et al., 2003) are sets of points that, for a specific camera position, are seen in a nearby viewpoint (at a radial distance less than 90 degrees) that are not in correspondence with silhouette-points of any (radially) closer viewpoint. What this definition informally means is that if we observe a suggestive contour in a specific viewing scenario, a silhouette will appear in that same area with a small change in the viewing position.

The processes described by DeCarlo et al. for suggestive contour extraction in object-space use a definition that relies on the directional derivative of the radial curvature of the surface. This has to be calculated from principal curvature values extracted from the object's surface, which are usually computed from the

Hessian of the potential function  $f(\mathbf{x})$  in an implicit. It is hard to find implicit representations that yield fast and numerically stable Hessian values and the MPU is no exception. It becomes particularly difficult to obtain these values near discontinuities, where it is highly probable to find a suggestive contour, because the potential function of the MPU is not well behaved. Therefore, our approach relies on another definition for suggestive contours mentioned by DeCarlo et al. in their image-space algorithm, namely the set of minima of the dot product between the view vector and the surface normal in the direction of the projection of the view vector onto the tangent plane at  $\mathbf{x}$ . This definition only requires evaluating gradient values  $\nabla f(\mathbf{x})$  from the implicit to obtain the surface normal.

Our suggestive contour extraction process begins with identifying the particles that lie in suggestive contour areas. We then form clusters of particles close to one another and apply line-fitting algorithms to each cluster to obtain the suggestive contours. In the next three sections we describe each of these methods in detail.

### 5.1 Identifying Suggestive Contour Particles

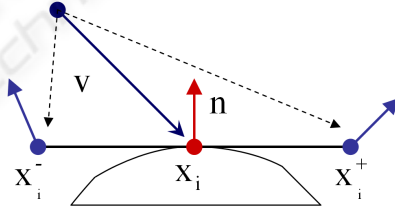


Figure 4: The positions  $\mathbf{x}_i^+$  and  $\mathbf{x}_i^-$  are calculated over the planar surface defined by  $\mathbf{n}$  and  $\mathbf{x}_i$ , in the direction of  $\mathbf{v}$ . The blue normal vectors are computed by consulting the gradient of the potential function in  $\mathbf{x}_i^+$  and  $\mathbf{x}_i^-$ .

The normalized view vector  $\mathbf{v}$  for a specific surface position  $\mathbf{x}$  and a view position  $\mathbf{c}$  is defined as:

$$\mathbf{v} = \frac{(\mathbf{x} - \mathbf{c})}{\|(\mathbf{x} - \mathbf{c})\|} \quad (3)$$

Consider  $\mathbf{w}$  as the projection of  $\mathbf{v}$  onto the surface tangent plane at  $\mathbf{x}$  with normal  $\mathbf{n}$ , obtained from the normalized gradient  $\nabla f(\mathbf{x})/\|\nabla f(\mathbf{x})\|$ . Suggestive contours can be defined as the set of minima of  $(\mathbf{n} \cdot \mathbf{v})$  in the direction of  $\mathbf{w}$  (DeCarlo et al., 2003).

Using this definition, we identify if a particle lies close to a suggestive contour by estimating if  $(\mathbf{n} \cdot \mathbf{v})$  experiences a local minimum at its position. Consider the two points  $\mathbf{x}_i^+$  and  $\mathbf{x}_i^-$  defined by:

$$\mathbf{x}_i^\pm = \mathbf{x}_i + k_d \mathbf{w} \quad (4)$$

$$\mathbf{x}_i^- = \mathbf{x}_i - k_d \mathbf{w} \quad (5)$$

where  $\mathbf{x}_i$  is the position of the particle  $P_i$  and  $k_d$  is scale-dependent and controls the displacement between  $\mathbf{x}_i^+$  and  $\mathbf{x}_i^-$  (for the tested models we usually use  $k_d = 0.5$ , Figure 4). Also consider that  $d_{p_i}$ ,  $d_{p_i^+}$  and  $d_{p_i^-}$  are the  $(\mathbf{n} \cdot \mathbf{v})$  values (obtained by consulting the gradient  $\nabla f(\mathbf{x})$ ) at  $\mathbf{x}_i$ ,  $\mathbf{x}_i^+$  and  $\mathbf{x}_i^-$  respectively). If the following inequalities are verified:

$$d_{p_i} < d_{p_i^+} \quad (6)$$

$$d_{p_i} < d_{p_i^-} \quad (7)$$

we can conclude that there is a local minimum between  $\mathbf{x}_i^+$  and  $\mathbf{x}_i^-$  and, if  $k_d$  is small enough,  $\mathbf{x}_i$  is a fair estimation of that minimum. Additionally we enforce the stability threshold mentioned in (DeCarlo et al., 2003), which excludes areas where the view vector is almost normal to the surface:

$$\theta_{sc} < \cos^{-1}(d_{p_i}) \quad (8)$$

where  $\theta_{sc}$  is a user-defined scalar. If the inequalities (6), (7) and (8) are verified, we consider that  $P_i$  belongs to a suggestive contour.

We use the minima of  $(\mathbf{n} \cdot \mathbf{v})$  to identify suggestive contour points in object-space, instead of the zeros of radial curvature that are used by DeCarlo et al., since the latter does not seem to work reliably on MPUs because it is discontinuous over blending functions. This is a new application of this definition for suggestive contours and it also allows for their extraction from implicit surfaces without using an auxiliary structure such as a polygonal mesh.

## 5.2 Clustering Points

After identifying suggestive contour particles, we cluster those particles that are close together on the surface. Our approach then builds a k-nearest neighbor graph of particles for each cluster. We start by taking one arbitrary particle  $P$  and searching for neighbors in 3D space within a fixed radius. This radius is multiplied by the  $\delta_i$  value of the respective octree cell to confine this search to a more limited space in areas of high curvature. From those nearby particles we select the  $k$  nearest (we normally use  $k = 3$ ) and those become the neighbors of  $P$  in the graph. For each neighbor we repeat the nearby particle search, skipping particles that have already been inspected. The cluster graph becomes complete when the search yields no new neighbors. We create additional clusters by applying this process to other particles that have not been inspected yet. Because of the dynamic nature of the search radius, it is possible to have particles from one cluster finding nearby particles from another cluster. In this situation we merge the two clusters.

## 5.3 Line Fitting

After clustering particles, we finally apply a line fitting algorithm to extract lines that represent each cluster topology. Our approach is inspired by the methods presented in (Gumhold et al., 2001) and starts by creating a minimum-spanning-tree (MST) of the cluster graph, using the optimized Kruskal algorithm. This process minimizes the geometric distance between points.

Since the obtained MST can have a large number of short branches, we must apply a simplification process to extract suggestive contour lines. To achieve this, we have two options. The first is to compute the longest path in the MST and use the corresponding edges as the suggestive contour. To find this path we take an arbitrary particle  $P$  and find the farthest particle  $P_f$  through breadth-first search. We then find the particle  $P'_f$  farthest from  $P_f$ . The longest path becomes the one connecting those two particles. The second approach is to trim the tree by removing short branches. To perform this trimming step, we go through all of the particles in the MST that have more than two connections to other particles (intersection nodes) and analyze each incident branch. If the branch leads to another intersection node, it remains intact. We remove the branch if it leads to a tree leaf node and is composed by less than  $k_{trim}$  (usually three) particles. In either approach, the extracted lines undergo a final smoothing step.

## 6 SILHOUETTES AND FEATURE LINES

As with the particle system, our silhouette and feature-line extraction methods are similar to (Foster et al., 2005) with four notable improvements. In what follows, we provide enough background to explain the base techniques and highlight our changes. To determine silhouettes, we start by identifying particles  $P_i$  with position  $\mathbf{x}_i$  that verify the following inequality:

$$|\mathbf{v}_i \cdot \mathbf{n}_i| < k_c \quad (9)$$

where  $k_c$  is controlled by the user (we use  $k_c = 0.05$  for the majority of the presented models),  $\mathbf{v}_i$  is the view vector and  $\mathbf{n}_i$  is the surface normal at  $\mathbf{x}_i$ . This inequality sets off a surface area where particles are considered to be close to the real silhouette (let's call it silhouette area).

From each identified particle we build the silhouette polyline iteratively by a numerical integration process. We use the predictor/corrector method pre-

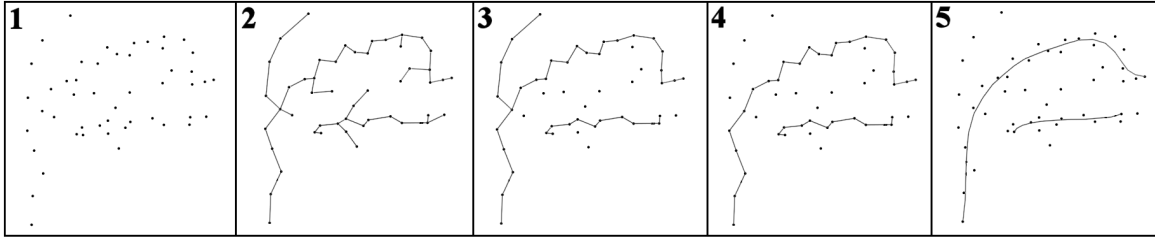


Figure 5: Extracting suggestive contours. 1: suggestive contour particles. 2: two clusters are identified and MSTs are built. 3: MST trimming approach. 4: MST longest-path approach. 5: using the longest-path approach and smoothing the lines, we obtain the suggestive contours.

sented by Foster et al., performing two point movements at each iteration. The first follows an estimated silhouette direction with a fixed step size, while the second results from two correction vectors computed to ensure that the line stays close to the silhouette and on the surface. Our approach uses a dynamic step size, by multiplying with the  $\delta_i$  value of the MPU octree cell (described in Section 4) where the point movement is taking place. This provides better precision to the silhouette polyline in areas of higher curvature, because the respective line segments become smaller, while improving performance in areas of lesser curvature, where the segments become larger (*Improvement 1*). The process stops if either (1) we detect that the silhouette is looping or (2) whenever it reaches the vicinity of another silhouette line or (3) when the following inequality is not verified:

$$|\mathbf{v}_i \cdot \mathbf{n}_i| < k_c \cdot k_e \quad (10)$$

This inequality is similar to (9), with the  $k_e$  parameter added, which expands the silhouette area where the curve may develop. By doing this, we can set a smaller  $k_c$  value to limit the number of identified silhouette particles and allow the silhouette building process to have a wider area of expansion (by using  $k_e = 2$  or  $k_e = 3$ ). Since it is very common to have particles that yield the same silhouette line, this technique improves the overall performance while maintaining quality and continuity of the extracted curves (*Improvement 2*). After all the silhouettes have been computed, we perform a 2D analysis to chain pairs of polylines that are within a certain distance of each other and follow similar orientation.

For feature-line extraction, we identify particles that lie in the relevant areas of the surface and build lines from their positions through numerical integration methods. We begin by discovering pairs of particles (straddle points) close to each other, which present a large difference between their surface normals. Foster et al. performed this step in the particle system simulation phase, by comparing the normal of each particle before and after its movement. Formally, for a certain particle  $P_i$  with initial surface normal  $\mathbf{n}_i$

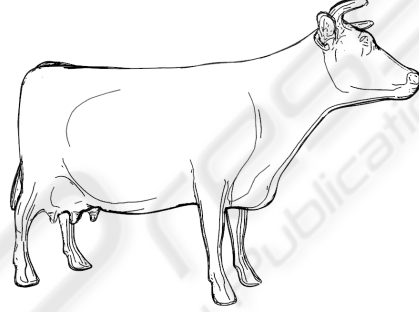


Figure 6: Silhouettes, Feature Lines and Suggestive Contours drawn over the Cow model.

and normal  $\mathbf{n}'_i$  after the movement, we consider the two respective positions  $\mathbf{x}_i$  and  $\mathbf{x}'_i$  to be straddle points if:

$$\text{angle}(\mathbf{n}_i, \mathbf{n}'_i) > k_a \quad (11)$$

where  $\text{angle}(\mathbf{v}_1, \mathbf{v}_2)$  returns the angle between two vectors and  $k_a$  is the threshold angle (we usually use  $k_a = 0.15$ ).

While this method is usually effective and extracts enough straddle points for a good visual result, there are situations where it may fail to find feature-lines due to our optimizations in the particle system. Indeed, particles which are initially set with near-optimal densities throughout the surface (see Section 4) can sometimes lead to a simulation stage where there will be very small changes in their positions. While this provides good performance, it may limit opportunities to identify straddle points. Therefore, we devised an alternative method to solve this problem which we apply when the Foster et al. method fails. It consists in searching for nearby points within a fixed radius of each particle and comparing normals to find pairs that verify Inequality (11) (*Improvement 3*).

After identifying straddle points, we move them along the respective faces separated by the feature, while trying to maintain a parallel direction to it. While this is performed, we estimate intermediate points that lie near the feature, to yield the feature



Figure 7: This caption has one line so it is centered.



Figure 8: The Phlegmatic Dragon model rendered using silhouettes, feature-lines and suggestive contours in our system.

polyline. As in the silhouette case, we use the  $\delta_i$  value of the current MPU octree cell to dynamically adjust the step of the movement to the local curvature (*Improvement 4*). The process stops when Inequality (11) is not verified or when another feature-line is detected in the vicinity of the straddle points.

## 7 RESULTS AND DISCUSSION

Our techniques for extracting silhouettes and feature-lines proved to be very effective as long as the MPU surface provides enough shape precision. This usually depends on the number and density of points in the object dataset. We are also able to produce suggestive contours for the objects, using our particle identification and line-fitting techniques.

For the two approaches that we used for fitting lines onto the suggestive contour MST (Section 5.3), the longest-path approach is guaranteed to extract single continuous line from each cluster, which makes it usually the best option to avoid artifacts caused by MST branching. However, when there are suggestive contours that almost intersect, the MST trim-

ming approach is usually able to correctly distinguish the intersecting lines when the respective clusters are merged together. This is in fact one of the major difficulties to overcome in the whole process: there is always a certain probability that two or more distinct suggestive contours will be covered by the same particle cluster because of their proximity. Therefore, we allow the user to select the appropriate method for each model.

Table 1: Performance results for our system. Each row indicates the model, number of points in the dataset, number of points in the particle system, frame-rate with silhouettes and feature-lines (in frames per second) and frame-rate with suggestive contours additionally.

Model	Dataset Points	Particle System	w/o Sugg. Contours	w/ Sugg. Contours
Bunny	69451	10000	3.4	1.9
Cow	92864	8334	3.4	1.8
Igea	268686	13665	3.7	1.4
Armadillo	345944	28360	1.6	0.5
Dragon	480076	26984	1.8	0.6
David	827181	59994	0.9	0.2

Table 1 presents the performance results obtained for the objects depicted in Figures 1, 6, 7, 8 and 9.



Figure 9: Renderings using silhouettes, feature-lines and suggestive contours. Left: The Igea model. Center: The Armadillo model. Right: The Armadillo model showing a particle distribution.

These results were gathered using a 3.6GHz Pentium IV with 2 gigabytes of RAM and a NVIDIA Quadro FX 3400 graphics card, running Windows XP SP2. All of the frame-rates were obtained after the particle system simulation process had been completed (usually the simulation comprises 20 iterations).

The number of particles in the particle-system is always determined by the MPU implicit structure, since we place one particle per octree cell. This strategy proved to be very effective for all of the tested models and also becomes automatic, without any need for the user to adjust the amount of particles needed for a correct surface coverage. As the results suggest, the number of particles is not proportional to the number of dataset points, because it is also influenced by the surface topology.

The performance results show that it is possible to achieve interactive frame-rates with medium complexity objects, even while extracting suggestive contours. However, the dimension of the particle system and the complexity of the model usually affect performance, since they influence the number of implicit function evaluations that are made and the associated computational overhead. This also explains why the suggestive contour extraction has such an influence on frame-rate, since it implies a great increase in function evaluations. Nevertheless, our approach compares favorably to (Foster et al., 2005) in that, for a similar frame-rate, we are usually able to render models with six times the number of particles, while including suggestive contours which are not handled by their approach. We should also mention that, while implicit-based approaches such as ours and the one from Foster et al. are currently less efficient than mesh-based ones, it is important to constantly improve these rendering methods because the descriptive flexibility that an implicit provides is vital in surface modeling and cannot be obtained when we use a polygonal mesh.

In terms of visual results, we verify that, for higher point densities in the dataset, the MPU can more accurately represent the surface and the overall line-

extracting process yields better results. This explains why the *David's Head* and *Dragon* models seem to present the most impressive depictions (Fig. 7 and 8).

There are however some important remarks to be made in terms of our system's limitations. Since many of our methods are based on Foster et al., we inherited some of the dependency on parameter setting by the user, namely in terms of adjusting the repulsion between particles and some silhouette extraction parameters to the scale and topology of the 3D model. Another limitation is the need for almost complete point clouds to achieve good results. These are usually obtained from 3D scanning of real objects and many times only certain portions of the overall surface are scanned. Although our particle system can deal with occasional holes in the MPU representation, it cannot effectively distribute points over an incomplete surface. Our technique also does not guarantee that all silhouettes, suggestive contours and feature lines are extracted from each surface, since the search for the relevant surface areas, for each viewing position, depends on the existence of strategically placed particles in those areas. This dependency is even more important for suggestive contours, since they are obtained from particle clusters. This results in unstable curves that become noticeable as the camera moves.

## 8 CONCLUSIONS AND FUTURE WORK

We have presented techniques to extract silhouettes, suggestive contours and feature-lines directly from MPU implicits, which are able to represent surfaces from large sets of points. Our methods benefit from the spatial information provided by the MPU structure, enabling us to automatically place particles throughout the surface and adjust the particle system and line extracting algorithms to the local shape. This implicit representation also provides good support for

shape modifications by allowing us to locally regenerate visual elements affected by edits. We improve on state of the art techniques for line-based rendering of implicits and introduce a method for suggestive contour extraction from this representation.

Our techniques provide precise and expressive depictions of very complex objects, especially the more detailed and complete datasets. Our results show better performance levels in comparison to similar systems for the same number of particles. Some areas for further improvement remain. Among them, new ways for defining the MPU implicit near the edge areas of the surface might allow us to draw more precise and continuous feature-lines. Some work also remains to be done to improve frame-coherent suggestive contours.

## ACKNOWLEDGEMENTS

The models are courtesy of the Digital Michelangelo Project 3D Model Repository (*David's Head*), the Stanford 3D Scanning Repository (*Bunny*, *Cow* and *Armadillo*), Cyberware (*Igea*) and UTIA, Academy of Sciences of the Czech Republic, and CGG, Czech Technical University in Prague (*Phlegmatic Dragon*).

## REFERENCES

- Barla, P., Thollot, J., and Sillion, F. (2005). Geometric clustering for line drawing simplification. In *Proc. of the Eurographics Symposium on Rendering*.
- Bloomenthal, J. (1997). *Introduction to Implicit Surfaces, First Edition (The Morgan Kaufmann Series in Computer Graphics)*. Morgan Kaufmann.
- Bremer, D. J. and Hughes, J. F. (1998). Rapid approximate silhouette rendering of implicit surfaces. In *Proc. of Implicit Surfaces '98*, pages 155–164.
- Burns, M., Klawe, J., Rusinkiewicz, S., Finkelstein, A., and DeCarlo, D. (2005). Line drawings from volume data. *ACM Trans. Graph.*, 24(3):512–518.
- de Araujo, B. R. and Jorge, J. A. P. (2004). Curvature dependent polygonization of implicit surfaces. In *Proc. of SIBGRAPI'04*, pages 266–273.
- DeCarlo, D., Finkelstein, A., and Rusinkiewicz, S. (2004). Interactive rendering of suggestive contours with temporal coherence. In *NPAR'04*, pages 15–24.
- DeCarlo, D., Finkelstein, A., Rusinkiewicz, S., and Santella, A. (2003). Suggestive contours for conveying shape. *ACM Trans. Graph. (Proc. SIGGRAPH)*, 22(3):848–855.
- Elber, G. (1998). Line art illustrations of parametric and implicit forms. *IEEE Trans. Vis. Comp. Graph.*, 4(1):71–81.
- Foster, K., Jepp, P., Wyvill, B., Sousa, M. C., Galbraith, C., and Jorge, J. A. (2005). Pen-and-ink for BlobTree implicit models. *Computer Graphics Forum*, 24(3):267–276.
- Gooch, B., Sloan, P.-P. J., Gooch, A., Shirley, P., and Riesenfeld, R. (1999). Interactive technical illustration. In *Proc. of the 1999 Symposium on Interactive 3D Graphics*, pages 31–38.
- Gumhold, S., Wang, X., and MacLeod, R. (2001). Feature extraction from point clouds. In *Proc. of the 10th International Meshing Roundtable*, pages 293–305.
- Isenberg, T., Freudenberg, B., Halper, N., Schlechtweg, S., and Strothotte, T. (2003). A developer's guide to silhouette algorithms for polygonal models. *IEEE Comput. Graph. Appl.*, 23(4):28–37.
- Jepp, P., Wyvill, B., and Sousa, M. C. (2006). Smarticles for sampling and rendering implicit models. *Theory and Practice of Computer Graphics 2006*, pages 39–46.
- Judd, T., Durand, F., and Adelson, E. H. (2007). Apparent ridges for line drawing. *ACM Trans. Graph.*, 26(3):19.
- Levet, F., Granier, X., and Schlick, C. (2006). Fast sampling of implicit surfaces by particle systems. In *Proc. of Shape Modeling International*, page 39.
- Ohtake, Y., Belyaev, A., Alexa, M., Turk, G., and Seidel, H.-P. (2003). Multi-level partition of unity implicits. *ACM Trans. Graph.*, 22(3):463–470.
- Pfister, H., Zwicker, M., van Baar, J., and Gross, M. (2000). Surfels: surface elements as rendering primitives. In *Proc. of SIGGRAPH '00*, pages 335–342.
- Plantinga, S. and Vegter, G. (2003). Contour generators of evolving implicit surfaces. In *SM '03: Proc. of the eighth ACM symposium on Solid modeling and applications*, pages 23–32.
- Proena, J., Jorge, J. A. P., and Sousa, M. C. (2007). Sampling point-set implicits. In *Eurographics Symposium on Point-Based Graphics*.
- Schmidt, R., Isenberg, T., and Wyvill, B. (2006). Interactive pen-and-ink rendering for implicit surfaces. In *ACM SIGGRAPH 2006 Conference Abstracts and Applications*. ACM Press.
- Sousa, M. C., Foster, K., Wyvill, B., and Samavati, F. (2003). Precise ink drawing of 3D models. *Computer Graphics Forum*, 22(3):369–379.
- van Overveld, K. and Wyvill, B. (2004). Shrinkwrap: An efficient adaptive algorithm for triangulating an isosurface. *The Visual Computer*, 20(6):362–379.
- Witkin, A. P. and Heckbert, P. S. (1994). Using particles to sample and control implicit surfaces. In *Proc. of SIGGRAPH '94*, pages 269–277.